

Observation of $\Xi(1620)^0$ and evidence for $\Xi(1690)^0$ in $\Xi_c^+ \rightarrow \Xi^- \pi^+ \pi^+$ decays

M. Sumihama,^{13,72} I. Adachi,^{19,15} J. K. Ahn,³⁹ H. Aihara,⁸⁷ S. Al Said,^{81,37} D. M. Asner,³ H. Atmacan,⁷⁷ T. Aushev,⁵⁴ R. Ayad,⁸¹ V. Babu,⁸² I. Badhrees,^{81,36} S. Bahinipati,²³ A. M. Bakich,⁸⁰ V. Bansal,⁶⁷ C. Beleño,¹⁴ M. Berger,⁷⁸ V. Bhardwaj,²² B. Bhuyan,²⁴ T. Bilka,⁵ J. Biswal,³⁴ G. Bonvicini,⁹¹ A. Bozek,⁶² M. Bračko,^{48,34} T. E. Browder,¹⁸ D. Červenkov,⁵ V. Chekelian,⁴⁹ A. Chen,⁵⁹ B. G. Cheon,¹⁷ K. Chilikin,⁴⁴ K. Cho,³⁸ S.-K. Choi,¹⁶ Y. Choi,⁷⁹ S. Choudhury,²⁵ D. Cinabro,⁹¹ S. Cunliffe,⁸ T. Czank,⁸⁵ N. Dash,²³ S. Di Carlo,⁴² Z. Doležal,⁵ T. V. Dong,^{19,15} Z. Drásal,⁵ S. Eidelman,^{4,65,44} D. Epifanov,^{4,65} J. E. Fast,⁶⁷ B. G. Fulsom,⁶⁷ R. Garg,⁶⁸ V. Gaur,⁹⁰ N. Gabyshev,^{4,65} A. Garmash,^{4,65} M. Gelb,³⁵ A. Giri,²⁵ P. Goldenzweig,³⁵ E. Guido,³² J. Haba,^{19,15} K. Hayasaka,⁶⁴ H. Hayashii,⁵⁸ S. Hirose,⁵⁵ W.-S. Hou,⁶¹ K. Inami,⁵⁵ G. Inguglia,⁸ A. Ishikawa,⁸⁵ R. Itoh,^{19,15} M. Iwasaki,⁶⁶ Y. Iwasaki,¹⁹ W. W. Jacobs,²⁷ H. B. Jeon,⁴¹ S. Jia,² Y. Jin,⁸⁷ K. K. Joo,⁶ T. Julius,⁵⁰ A. B. Kaliyar,²⁶ K. H. Kang,⁴¹ G. Karyan,⁸ Y. Kato,⁵⁶ C. Kiesling,⁴⁹ D. Y. Kim,⁷⁶ J. B. Kim,³⁹ K. T. Kim,³⁹ S. H. Kim,¹⁷ K. Kinoshita,⁷ P. Kodyš,⁵ S. Korpar,^{48,34} D. Kotchetkov,¹⁸ P. Križan,^{45,34} R. Kroeger,⁵¹ P. Krokovny,^{4,65} R. Kumar,⁷¹ A. Kuzmin,^{4,65} Y.-J. Kwon,⁹³ J. S. Lange,¹² I. S. Lee,¹⁷ S. C. Lee,⁴¹ L. K. Li,²⁸ Y. B. Li,⁶⁹ L. Li Gioi,⁴⁹ J. Libby,²⁶ D. Liventsev,^{90,19} M. Lubej,³⁴ T. Luo,¹¹ M. Masuda,⁸⁶ T. Matsuda,⁵² D. Matvienko,^{4,65,44} M. Merola,^{31,57} K. Miyabayashi,⁵⁸ H. Miyata,⁶⁴ R. Mizuk,^{44,53,54} G. B. Mohanty,⁸² H. K. Moon,³⁹ T. Mori,⁵⁵ R. Mussa,³² E. Nakano,⁶⁶ T. Nakano,⁷² M. Nakao,^{19,15} T. Nanut,³⁴ K. J. Nath,²⁴ Z. Natkaniec,⁶² M. Niiyama,⁴⁰ N. K. Nisar,⁷⁰ S. Nishida,^{19,15} H. Ono,^{63,64} P. Pakhlov,^{44,53} G. Pakhlova,^{44,54} B. Pal,³ S. Pardi,³¹ H. Park,⁴¹ S. Paul,⁸⁴ T. K. Pedlar,⁴⁷ R. Pestotnik,³⁴ L. E. Piilonen,⁹⁰ V. Popov,^{44,54} M. Ritter,⁴⁶ G. Russo,³¹ D. Sahoo,⁸² S. Sandilya,⁷ L. Santelj,¹⁹ T. Sanuki,⁸⁵ V. Savinov,⁷⁰ O. Schneider,⁴³ G. Schnell,^{1,21} C. Schwanda,²⁹ Y. Seino,⁶⁴ K. Senyo,⁹² M. E. Seviar,⁵⁰ V. Shebalin,^{4,65} C. P. Shen,² T.-A. Shibata,⁸⁸ J.-G. Shiu,⁶¹ B. Shwartz,^{4,65} F. Simon,^{49,83} A. Sokolov,³⁰ E. Solovieva,^{44,54} M. Starič,³⁴ J. F. Strube,⁶⁷ T. Sumiyoshi,⁸⁹ M. Takizawa,^{75,20,73} U. Tamponi,³² K. Tanida,³³ N. Taniguchi,¹⁹ F. Tenchini,⁵⁰ M. Uchida,⁸⁸ T. Uglov,^{44,54} S. Uno,^{19,15} P. Urquijo,⁵⁰ S. E. Vahsen,¹⁸ C. Van Hulse,¹ G. Varner,¹⁸ V. Vorobyev,^{4,65,44} A. Vossen,⁹ B. Wang,⁷ C. H. Wang,⁶⁰ M.-Z. Wang,⁶¹ P. Wang,²⁸ X. L. Wang,¹¹ M. Watanabe,⁶⁴ S. Watanuki,⁸⁵ E. Widmann,⁷⁸ E. Won,³⁹ H. Ye,⁸ J. Yelton,¹⁰ C. Z. Yuan,²⁸ Y. Yusa,⁶⁴ S. Zakharov,^{44,54} Z. P. Zhang,⁷⁴ V. Zhilich,^{4,65} V. Zhukova,^{44,53} and V. Zhulanov^{4,65}

(The Belle Collaboration)

¹University of the Basque Country UPV/EHU, 48080 Bilbao

²Beihang University, Beijing 100191

³Brookhaven National Laboratory, Upton, New York 11973

⁴Budker Institute of Nuclear Physics SB RAS, Novosibirsk 630090

⁵Faculty of Mathematics and Physics, Charles University, 121 16 Prague

⁶Chonnam National University, Kwangju 660-701

⁷University of Cincinnati, Cincinnati, Ohio 45221

⁸Deutsches Elektronen-Synchrotron, 22607 Hamburg

⁹Duke University, Durham, North Carolina 27708

¹⁰University of Florida, Gainesville, Florida 32611

¹¹Key Laboratory of Nuclear Physics and Ion-beam Application (MOE) and Institute of Modern Physics, Fudan University, Shanghai 200443

¹²Justus-Liebig-Universität Gießen, 35392 Gießen

¹³Gifu University, Gifu 501-1193

¹⁴II. Physikalisches Institut, Georg-August-Universität Göttingen, 37073 Göttingen

¹⁵SOKENDAI (The Graduate University for Advanced Studies), Hayama 240-0193

¹⁶Gyeongsang National University, Chinju 660-701

¹⁷Hanyang University, Seoul 133-791

¹⁸University of Hawaii, Honolulu, Hawaii 96822

¹⁹High Energy Accelerator Research Organization (KEK), Tsukuba 305-0801

²⁰J-PARC Branch, KEK Theory Center, High Energy Accelerator Research Organization (KEK), Tsukuba 305-0801

²¹IKERBASQUE, Basque Foundation for Science, 48013 Bilbao

²²Indian Institute of Science Education and Research Mohali, SAS Nagar, 140306

²³Indian Institute of Technology Bhubaneswar, Satya Nagar 751007

²⁴Indian Institute of Technology Guwahati, Assam 781039

²⁵Indian Institute of Technology Hyderabad, Telangana 502285

- ²⁶Indian Institute of Technology Madras, Chennai 600036
²⁷Indiana University, Bloomington, Indiana 47408
²⁸Institute of High Energy Physics, Chinese Academy of Sciences, Beijing 100049
²⁹Institute of High Energy Physics, Vienna 1050
³⁰Institute for High Energy Physics, Protvino 142281
³¹INFN - Sezione di Napoli, 80126 Napoli
³²INFN - Sezione di Torino, 10125 Torino
³³Advanced Science Research Center, Japan Atomic Energy Agency, Naka 319-1195
³⁴J. Stefan Institute, 1000 Ljubljana
³⁵Institut für Experimentelle Teilchenphysik, Karlsruher Institut für Technologie, 76131 Karlsruhe
³⁶King Abdulaziz City for Science and Technology, Riyadh 11442
³⁷Department of Physics, Faculty of Science, King Abdulaziz University, Jeddah 21589
³⁸Korea Institute of Science and Technology Information, Daejeon 305-806
³⁹Korea University, Seoul 136-713
⁴⁰Kyoto University, Kyoto 606-8502
⁴¹Kyungpook National University, Daegu 702-701
⁴²LAL, Univ. Paris-Sud, CNRS/IN2P3, Université Paris-Saclay, Orsay
⁴³École Polytechnique Fédérale de Lausanne (EPFL), Lausanne 1015
⁴⁴P.N. Lebedev Physical Institute of the Russian Academy of Sciences, Moscow 119991
⁴⁵Faculty of Mathematics and Physics, University of Ljubljana, 1000 Ljubljana
⁴⁶Ludwig Maximilians University, 80539 Munich
⁴⁷Luther College, Decorah, Iowa 52101
⁴⁸University of Maribor, 2000 Maribor
⁴⁹Max-Planck-Institut für Physik, 80805 München
⁵⁰School of Physics, University of Melbourne, Victoria 3010
⁵¹University of Mississippi, University, Mississippi 38677
⁵²University of Miyazaki, Miyazaki 889-2192
⁵³Moscow Physical Engineering Institute, Moscow 115409
⁵⁴Moscow Institute of Physics and Technology, Moscow Region 141700
⁵⁵Graduate School of Science, Nagoya University, Nagoya 464-8602
⁵⁶Kobayashi-Maskawa Institute, Nagoya University, Nagoya 464-8602
⁵⁷Università di Napoli Federico II, 80055 Napoli
⁵⁸Nara Women's University, Nara 630-8506
⁵⁹National Central University, Chung-li 32054
⁶⁰National United University, Miao Li 36003
⁶¹Department of Physics, National Taiwan University, Taipei 10617
⁶²H. Niewodniczanski Institute of Nuclear Physics, Krakow 31-342
⁶³Nippon Dental University, Niigata 951-8580
⁶⁴Niigata University, Niigata 950-2181
⁶⁵Novosibirsk State University, Novosibirsk 630090
⁶⁶Osaka City University, Osaka 558-8585
⁶⁷Pacific Northwest National Laboratory, Richland, Washington 99352
⁶⁸Panjab University, Chandigarh 160014
⁶⁹Peking University, Beijing 100871
⁷⁰University of Pittsburgh, Pittsburgh, Pennsylvania 15260
⁷¹Punjab Agricultural University, Ludhiana 141004
⁷²Research Center for Nuclear Physics, Osaka University, Osaka 567-0047
⁷³Theoretical Research Division, Nishina Center, RIKEN, Saitama 351-0198
⁷⁴University of Science and Technology of China, Hefei 230026
⁷⁵Showa Pharmaceutical University, Tokyo 194-8543
⁷⁶Soongsil University, Seoul 156-743
⁷⁷University of South Carolina, Columbia, South Carolina 29208
⁷⁸Stefan Meyer Institute for Subatomic Physics, Vienna 1090
⁷⁹Sungkyunkwan University, Suwon 440-746
⁸⁰School of Physics, University of Sydney, New South Wales 2006
⁸¹Department of Physics, Faculty of Science, University of Tabuk, Tabuk 71451
⁸²Tata Institute of Fundamental Research, Mumbai 400005
⁸³Excellence Cluster Universe, Technische Universität München, 85748 Garching
⁸⁴Department of Physics, Technische Universität München, 85748 Garching
⁸⁵Department of Physics, Tohoku University, Sendai 980-8578
⁸⁶Earthquake Research Institute, University of Tokyo, Tokyo 113-0032
⁸⁷Department of Physics, University of Tokyo, Tokyo 113-0033
⁸⁸Tokyo Institute of Technology, Tokyo 152-8550

⁸⁹Tokyo Metropolitan University, Tokyo 192-0397

⁹⁰Virginia Polytechnic Institute and State University, Blacksburg, Virginia 24061

⁹¹Wayne State University, Detroit, Michigan 48202

⁹²Yamagata University, Yamagata 990-8560

⁹³Yonsei University, Seoul 120-749

We report the first observation of the doubly-strange baryon $\Xi(1620)^0$ in its decay to $\Xi^-\pi^+$ via $\Xi_c^+ \rightarrow \Xi^-\pi^+\pi^+$ decays based on a 980 fb^{-1} data sample collected with the Belle detector at the KEKB asymmetric-energy e^+e^- collider. The mass and width are measured to be 1610.4 ± 6.0 (stat) $_{-3.5}^{+5.9}$ (syst) MeV/c^2 and 59.9 ± 4.8 (stat) $_{-3.0}^{+2.8}$ (syst) MeV , respectively. We obtain 4.0σ evidence of the $\Xi(1690)^0$ with the same data sample. These results shed light on the structure of hyperon resonances with strangeness $S = -2$.

PACS numbers: 13.66.Bc, 14.20.Jn

The constituent quark model has been very successful in describing the ground state of the flavor SU(3) octet and decuplet baryons [1–3]. However, some observed excited states do not agree well with the theoretical prediction. It is thus important to study such unusual states, both to probe the limitation of the quark models and to spot unrevealed aspects of the quantum-chromodynamics(QCD) description of the structure of hadron resonances. Intriguingly, the Ξ resonances with strangeness $S = -2$ may provide important information on the latter aspect.

The quantum numbers of several nucleons and $S = -1$ hyperon resonances have been measured. Recently, there has been significant progress in the experimental study of charmed baryons by the Belle, BaBar, and LHCb collaborations. In contrast, only a small number of Ξ states have been measured [1]. Neither the first radial excitation with the spin-parity of $J^P = \frac{1}{2}^+$ nor a first orbital excitation with $J^P = \frac{1}{2}^-$ has been identified. Determination of the mass of the first excited state is a vital test of our understanding of the structure of Ξ resonances. One candidate for the first excited state is the $\Xi(1690)$, which has a three-star rating on a four-star scale [1]. Another candidate is the $\Xi(1620)$, with a one-star rating [1]. If the $\frac{1}{2}^-$ state is found, it will be the doubly-strange analogue to the $\Lambda(1405)$ state, which has been postulated as a candidate meson-baryon molecular state or a pentaquark [4].

Experimental evidence for the $\Xi(1620) \rightarrow \Xi\pi$ decay was reported in K^-p interactions in the 1970's [5–7]. The mass and width measurements are consistent but have large statistical uncertainties. The most recent experiment, in 1981, has not seen this resonance [8]. There is a lingering theoretical controversy about the interpretation of the $\Xi(1620)$ and $\Xi(1690)$ states [9–16], extending from their assignment in the quark model to their existence. This would be addressed with new high-quality experimental results for the first excited state with $S = -2$. The hadronic decays of charmed baryons governed by the $c \rightarrow s$ quark transition are a good laboratory to probe these strange baryons.

In this Letter, we study the decay $\Xi_c^+ \rightarrow \Xi^*\pi^+, \Xi^{*0} \rightarrow$

$\Xi^-\pi^+$ based on a data sample collected with the Belle detector at the KEKB asymmetric-energy e^+e^- (3.5 on 8 GeV) collider [17]. The charge conjugate mode is included throughout this Letter. The sample corresponds to an integrated luminosity of 980 fb^{-1} . The major part of the data was taken at the $\Upsilon(4S)$ resonance; in addition, smaller integrated luminosity samples were collected off resonance and at the $\Upsilon(1S)$, $\Upsilon(2S)$, $\Upsilon(3S)$, and $\Upsilon(5S)$. We use a Monte Carlo simulation (MC) sample to characterize the mass resolution, detector acceptance, and invariant mass distribution in the available phase space. The MC samples are generated with EVTGEN [18], and the detector response is simulated with GEANT3 [19].

The Belle detector is a large-solid-angle magnetic spectrometer that consists of a silicon vertex detector (SVD), a 50-layer central drift chamber (CDC), an array of aerogel threshold Cherenkov counters (ACC), a barrel-like arrangement of time-of-flight scintillation counters (TOF), and an electromagnetic calorimeter comprised of CsI(Tl) crystals (ECL); all these components are located inside a superconducting solenoid coil that provides a 1.5 T magnetic field. The detector is described in detail elsewhere [20]. Two inner detector configurations were used. A 2.0 cm radius beampipe and a 3-layer SVD was used for the first sample of 156 fb^{-1} , while a 1.5 cm radius beampipe, a 4-layer SVD and a small-cell inner CDC were used to record the remaining 824 fb^{-1} [21].

We reconstruct the Ξ_c^+ via the $\Xi_c^+ \rightarrow \Xi^-\pi^+\pi^+$, $\Xi^- \rightarrow \Lambda\pi^-$, $\Lambda \rightarrow p\pi^-$ decay channel. Final-state charged particles, p and π^\pm , are identified using the information from the tracking (SVD, CDC) and charged-hadron identification (CDC, ACC, TOF) systems combined into likelihood ratios $\mathcal{L}(i : j) = \mathcal{L}_i / (\mathcal{L}_i + \mathcal{L}_j)$, where $i, j \in \{p, K, \pi\}$. The π^\pm particles are selected by requiring the likelihood ratios $\mathcal{L}(\pi : K) > 0.6$; this has about 90% efficiency. The likelihood ratios $\mathcal{L}(p : \pi) > 0.6$ and $\mathcal{L}(p : K) > 0.6$ are required for proton candidates from the Λ . The Λ particles are reconstructed from $p\pi^-$ pairs with about 98% efficiency. The three-momentum of the Λ is combined with that of a π^- track to reconstruct the helix trajectory of the Ξ^- candidate; this helix is extrapo-

lated back toward the IP. A vertex fit is applied to the $\Xi^- \rightarrow \Lambda\pi^-$ decay and the χ^2 is required to be less than 50. We retain Ξ^- candidates whose mass is within $\pm 3.0 \text{ MeV}/c^2$ ($\pm 3\sigma$) of the nominal Ξ^- mass. Then, we combine the Ξ^- with two π^+ candidates, where the pion with the lower (higher) momentum is labeled π_L^+ (π_H^+). The closest distance between the π^+ track and the nominal e^+e^- interaction point must satisfy $|dz| < 1.3 \text{ cm}$ along the beam direction, and $|dr| < 0.16$ (0.13) cm in the transverse plane for π_L^+ (π_H^+) for both π_L^+ and π_H^+ . A vertex fit is applied to the $\Xi_c^+ \rightarrow \Xi^- \pi^+ \pi^+$ decay. The χ^2 is required to be less than 50. To purify the Ξ_c^+ samples, the scaled momentum $x_p = p_{CM}/\sqrt{\frac{1}{4}s - m(\Xi_c^+)^2}$ is required to exceed 0.5, where p_{CM} is the momentum of Ξ_c^+ in the e^+e^- center-of-mass system, s is the squared total center-of-mass energy, and $m(\Xi_c^+)$ is the Ξ_c^+ nominal mass. We retain Ξ_c^+ candidates that satisfy $|M(\Xi^- \pi^+ \pi^+) - m(\Xi_c^+)| < 12.7 \text{ MeV}/c^2$. The region $30.0 \text{ MeV}/c^2 < |M(\Xi^- \pi^+ \pi^+) - m(\Xi_c^+)| < 55.4 \text{ MeV}/c^2$ defines the sideband for estimation of the combinatorial background.

The $M(\Xi^- \pi_L^+)$ and $M(\Xi^- \pi_H^+)$ distributions of the final sample are shown in Fig. 1(a). Peaks corresponding to $\Xi(1530)^0$, $\Xi(1620)^0$, and $\Xi(1690)^0$ are observed in the $M(\Xi^- \pi_L^+)$ distribution. A reflection due to $\Xi(1530)^0$ decays is seen around $2.2 \text{ GeV}/c^2$ in $M(\Xi^- \pi_H^+)$. The hatched histograms are the distributions of the Ξ_c^+ sideband events, where only the $\Xi(1530)^0$ is observed. The Dalitz plot of $M^2(\Xi^- \pi_L^+)$ vs. $M^2(\Xi^- \pi_H^+)$ is shown in Fig. 1(b). The cluster of events due to the $\Xi(1530)^0$ is seen. The region $4.3 - 5.3 (\text{GeV}/c^2)^2$ in $M^2(\Xi^- \pi_H^+)$ contains the $\Xi(1620)^0$ and $\Xi(1690)^0$ signals. There are currently no known particles with a mass in the range of $2.1 - 2.3 \text{ GeV}/c^2$ that would decay into $\Xi\pi$. Such massive particles would decay predominantly into a three-particles final state such as $\Xi\pi\pi$. The peaks around 1.60 and $1.69 \text{ GeV}/c^2$ in $M(\Xi^- \pi_L^+)$ are interpreted as the $\Xi(1620)^0$ and $\Xi(1690)^0$ resonances. We see an unknown structure in the range $1.8 - 2.1 \text{ GeV}/c^2$ in $M(\Xi^- \pi^+)$. These events are expected to be due to resonances such as $\Xi(1820)^0$, $\Xi(1950)^0$, and $\Xi(2030)^0$.

The correction of the event-reconstruction efficiency is applied to the mass spectrum. To calculate this efficiency, we generate MC events for the non-resonant three-body decay $\Xi_c^+ \rightarrow \Xi^- \pi^+ \pi^+$ with a uniform distribution in phase space. The efficiency is the number of events surviving the selections divided by the total number of generated events, and is measured as a function of $M(\Xi^- \pi_L^+)$; the resulting efficiency is from 0.082 to 0.097 and shows a nearly flat distribution in $M(\Xi^- \pi_L^+)$. The mass distribution is divided by this efficiency and is normalized by the total number of events.

We perform a binned maximum-likelihood fit to the efficiency-corrected $M(\Xi^- \pi_L^+)$ distribution. The fit is applied for the data samples in the signal region and the

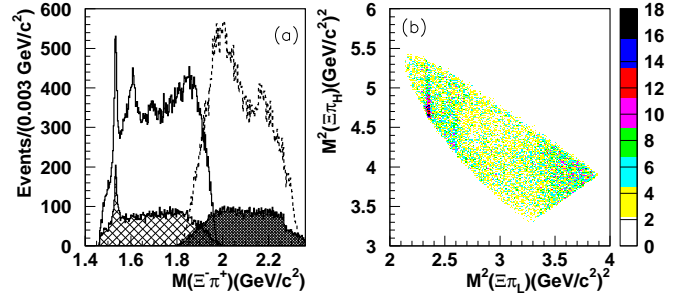


FIG. 1: (a) The $\Xi^- \pi_L^+$ (solid) and $\Xi^- \pi_H^+$ (dashed) invariant mass distributions in the Ξ_c^+ signal region, as well as the corresponding distributions (hatched) in Ξ_c^+ sideband region. (b) The Dalitz distribution for $\Xi_c^+ \rightarrow \Xi^- \pi_H^+ \pi_L^+$. (color online)

sideband region simultaneously. The fitting range is restricted to $(1.46, 1.76) \text{ GeV}/c^2$ to avoid inclusion of the unknown structure between 1.8 and $2.1 \text{ GeV}/c^2$. The fitting function for the mass spectrum in the signal region includes resonances due to the $\Xi(1530)^0$, $\Xi(1620)^0$, and $\Xi(1690)^0$, a non-resonant contribution, and the combinatorial background. The fitting function for the mass spectrum in the sideband region includes the $\Xi(1530)^0$ signal and the combinatorial background. The shape of the fitting function for the combinatorial backgrounds is common for the mass spectra in the signal region and the sideband region, and is made by a function with a threshold: $u^a \exp(ub) + cu$, where $u = 1 - [(2 - M)/(2 - d)]^2$ and $M = M(\Xi^- \pi_L^+)$; a, b, c , and d are free parameters. We assume an S-wave non-resonant contribution, and generate the distribution from the MC simulation of $\Xi_c^+ \rightarrow \Xi^- \pi^+ \pi^+$ decays with a uniform distribution in phase space. The $\Xi(1620)^0$ signal is modeled with the S-wave relativistic Breit-Wigner function. The interference between $\Xi(1620)^0$ and the S-wave non-resonant process is taken into account, and these are coherently added. The $\Xi(1530)^0$ and $\Xi(1690)^0$ signals are modeled with P- and S-wave relativistic Breit-Wigner functions convolved with a fixed Gaussian resolution function of width $1.38 \text{ MeV}/c^2$ and $2.04 \text{ MeV}/c^2$, respectively, as determined from the MC simulation. The width and mass of $\Xi(1530)^0$ and $\Xi(1620)^0$ particles are floated in the fit. The mass and width of the $\Xi(1690)^0$ are fixed in the fit to the values $(1686 \text{ MeV}/c^2$ and 10 MeV , respectively) measured by the WA89 Collaboration [22]. Figure 2(a) shows the $\Xi^- \pi_L^+$ mass spectrum with the fitting result. The χ^2/ndf (where ndf is the number of degrees of freedom) is $66/86$. For the $\Xi(1690)^0$ resonance, the fit is repeated by fixing the yield to zero; the resulting difference in log-likelihood with respect to the nominal fit and the change of the number of degrees of freedom are used to obtain the signal significance. The statistical significance of the $\Xi(1690)^0$ is 4.5σ . To check the stability of

the significance of the $\Xi(1690)^0$, various fit conditions are tried. When the P-wave-only relativistic Breit-Wigner with fixed mass and width is used as the fitting function, the significance is 4.0σ . When the S-wave-only relativistic Breit-Wigner with the floated mass and width is used, the significance is 4.6σ . We take the minimum value of 4.0σ as the significance including the systematic uncertainty. The measured mass and width of $\Xi(1530)^0$ are $1533.4 \pm 0.35 \text{ MeV}/c^2$ and $11.2 \pm 1.5 \text{ MeV}$, respectively. The measured mass and width of $\Xi(1620)^0$ are $1610.4 \pm 6.0 \text{ MeV}/c^2$ and $60.0 \pm 4.8 \text{ MeV}$, respectively. The mass resolution (σ) at $1600 \text{ MeV}/c^2$ is $1.6 \text{ MeV}/c^2$ as determined from the MC simulation. The width of the $\Xi(1620)^0$ is 59.9 MeV after incorporating this mass resolution.

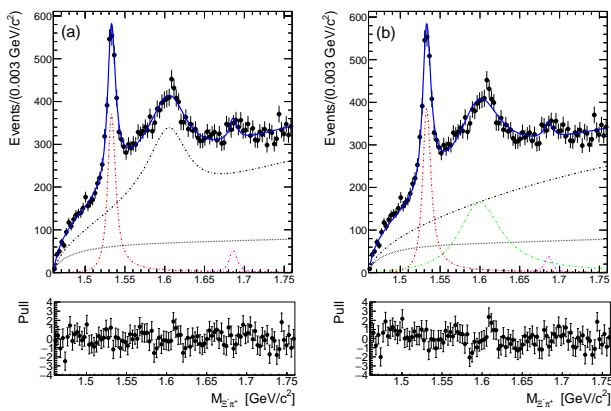


FIG. 2: (a) The $\Xi^-\pi_L^+$ invariant mass spectrum (points with error bars), together with the fit result (solid blue curve) including the following components: $\Xi(1530)^0$ signal (dashed red curve), $\Xi(1690)^0$ signal (dot-dashed pink curve), $\Xi(1620)^0$ signal and non-resonant contribution (dot-dashed black curve), the combinatorial backgrounds (dotted black curve). The bottom plots show the normalized residuals (pulls) of the fits. (b) The fit without the interference between $\Xi(1620)^0$ and the S-wave non-resonant process. The dot-dashed black curve represents the S-wave non-resonant process and the dot-dashed green curve represents the $\Xi(1620)^0$. (color online)

We itemize the systematic uncertainties on the mass and width of the $\Xi(1620)^0$ resonance in Table I. The mass scale and width is checked by comparing the reconstructed mass of the $\Xi(1530)^0$ in the $\Xi^-\pi^+$ channel with the nominal mass. The differences of the mass and width are $-1.5 \text{ MeV}/c^2$ and -2.7 MeV , respectively. We then generate and simulate $\Xi_c^+ \rightarrow \Xi^*\pi^+$, $\Xi^* \rightarrow \Xi^-\pi^+$ events and analyze these events by the same program as for the real data; the mass scale is checked by comparing the reconstructed mass of Ξ^* with the generated mass. Here, the difference of the mass is $-0.2 \text{ MeV}/c^2$ and the difference of the width is less than the statistical error. The systematic uncertainty due to the mass shape of the $\Xi(1620)^0$ is obtained by applying the fit with the P-wave

relativistic Breit-Wigner function instead of the S-wave function. The systematic error due to the mass shape of the $\Xi(1690)^0$ is obtained by applying the fit with the P-wave relativistic Breit-Wigner function instead of the S-wave function, with floated mass and width. The nominal bin width of the mass spectrum is $3.0 \text{ MeV}/c^2$. We determine its systematic uncertainty by changing the bin size from 2.5 to $3.5 \text{ MeV}/c^2$ and refitting.

All of the above sources are uncorrelated, so the total systematic uncertainty is calculated by summing them in quadrature.

TABLE I: Systematic uncertainties for the mass and the width of $\Xi(1620)^0$.

Source	Mass (MeV/c^2)	Width (MeV)
Mass scale	-1.5	-2.7
Mass shape of $\Xi(1620)$	+4.5	+1.8
Mass shape of $\Xi(1690)$	+2.3	+1.7
Bin size	± 3.1	± 1.3
Total	$+5.9$ -3.5	$+2.8$ -3.0

We refit the data using a function that excludes the interference between $\Xi(1620)^0$ and the S-wave non-resonant process. Figure 2(b) shows the $\Xi^-\pi_L^+$ mass spectrum with this hypothesis. The χ^2/ndf is $80/87$, which is worse than for the nominal fit. Here, the measured mass and width of the $\Xi(1620)^0$ are $1601.2 \pm 1.5 \text{ MeV}/c^2$ and $63.6 \pm 8.7 \text{ MeV}$, respectively.

For the first time, the $\Xi(1620)^0$ particle is observed in its decay to $\Xi^-\pi^+$ via $\Xi_c^+ \rightarrow \Xi^-\pi^+\pi^+$ decays. The number of $\Xi(1620)^0$ events is two orders of magnitude larger than in previous experiments. The measured mass and width of the $\Xi(1620)^0$ are consistent with the results of previous measurements within the large uncertainties of the latter and are much more precise. The width of the $\Xi(1620)^0$ is somewhat larger than that of the other Ξ^* particles [1].

The constituent quark models have predicted the first excited states of Ξ around $1800 \text{ MeV}/c^2$ [3]; therefore, it is difficult to explain the structure of the $\Xi(1620)^0$ and $\Xi(1690)^0$ in this context. Instead, it implies that these states are candidates of a new class of exotic hadrons. We observe in the low-mass region two states with a mass difference of about $80 \text{ MeV}/c^2$: the $\Xi(1620)^0$ is strongly coupled to $\Xi\pi$ and the $\Xi(1690)^0$ to ΣK . The situation is similar to the two poles of the $\Lambda(1405)$ [4] and suggests the possibility of two poles in the $S = -2$ sector. Studying these states may explain the riddle about the $\Lambda(1405)$; consequently, the interplay between the $S = -1$ and $S = -2$ states can help resolve this longstanding problem of hadron physics.

The $\Xi(1620)^0$ and $\Xi(1690)^0$ particles are found in the decay of Ξ_c^+ while their signals are not seen in the side-band events of Fig.1(a). These results offer a clue for

understanding the quark structure of these exotic states. The result indicates that the hadronic decays of charmed baryons via charm-to-strange quark transitions are potentially a promising system for further studies of strange baryons [16].

We thank the KEKB group for the excellent operation of the accelerator; the KEK cryogenics group for the efficient operation of the solenoid; and the KEK computer group, and the Pacific Northwest National Laboratory (PNNL) Environmental Molecular Sciences Laboratory (EMSL) computing group for strong computing support; and the National Institute of Informatics, and Science Information NETwork 5 (SINET5) for valuable network support. We acknowledge support from the Ministry of Education, Culture, Sports, Science, and Technology (MEXT) of Japan, the Japan Society for the Promotion of Science (JSPS), and the Tau-Lepton Physics Research Center of Nagoya University; the Australian Research Council including grants DP180102629, DP170102389, DP170102204, DP150103061, FT130100303; Austrian Science Fund under Grant No. P 26794-N20; the National Natural Science Foundation of China under Contracts No. 11435013, No. 11475187, No. 11521505, No. 11575017, No. 11675166, No. 11705209; Key Research Program of Frontier Sciences, Chinese Academy of Sciences (CAS), Grant No. QYZDJ-SSW-SLH011; the CAS Center for Excellence in Particle Physics (CCEPP); the Shanghai Pujiang Program under Grant No. 18PJ1401000; the Ministry of Education, Youth and Sports of the Czech Republic under Contract No. LTT17020; the Carl Zeiss Foundation, the Deutsche Forschungsgemeinschaft, the Excellence Cluster Universe, and the VolkswagenStiftung; the Department of Science and Technology of India; the Istituto Nazionale di Fisica Nucleare of Italy; National Research Foundation (NRF) of Korea Grants No. 2015H1A2A1033649, No. 2016R1D1A1B01010135, No. 2016K1A3A7A09005 603, No. 2016R1D1A1B02012900, No. 2018R1A2B3003 643, No. 2018R1A6A1A06024970, No. 2018R1D1A1B07047294; Radiation Science Research Institute, Foreign Large-size Research Facility Application Supporting project, the Global Science Experimental Data Hub Center of the Korea Institute of Science and Technology Information and KREONET/GLORIAD; the Polish Ministry of Science and Higher Education and the National Science Center; the Grant of the Russian Feder-

ation Government, Agreement No. 14.W03.31.0026; the Slovenian Research Agency; Ikerbasque, Basque Foundation for Science, Basque Government (No. IT956-16) and Ministry of Economy and Competitiveness (MINECO) (Juan de la Cierva), Spain; the Swiss National Science Foundation; the Ministry of Education and the Ministry of Science and Technology of Taiwan; and the United States Department of Energy and the National Science Foundation.

-
- [1] M. Tanabashi et al. (Particle Data Group), *Phys. Rev. D* **98** 030001 (2018).
 - [2] K. T. Chao, N. Isgur, and G. Karl, *Phys. Rev. D* **23** 155 (1981).
 - [3] S. Capstick and N. Isgur, *Phys. Rev. D* **34** 2809 (1986).
 - [4] T. Hyodo and D. Jido, *Prog. Part. Nucl. Phys.* **67** 55 (2012).
 - [5] E. Briefel *et al.*, *Phys. Rev. D* **16** 2706 (1977).
 - [6] A. de Bellefon *et al.*, *Nuovo Cimento* **28** 289 (1975).
 - [7] R. T. Ross *et al.*, *Phys. Lett. B* **38** 177 (1972).
 - [8] J. K. Hassall *et al.*, *Nucl. Phys. B* **189** 397 (1981).
 - [9] U. Loring, B. Ch. Metsch, and H. R. Petry, *Eur. Phys. J. A* **10** 447 (2001).
 - [10] A. Ramos, E. Oset, and C. Bennhold, *Phys. Rev. Lett.* **25** 252001 (2002).
 - [11] C. Garcia-Recio, M. F. M. Lutz, and J. Nieves, *Phys. Lett. B* **582** 49 (2004).
 - [12] Y. Oh, *Phys. Rev. D* **75** 074002 (2007).
 - [13] M. Pervin and W. Roberts, *Phys. Rev. C* **77** 025202 (2008).
 - [14] L.Y. Xiao and X.H. Zhong, *Phys. Rev. D* **87** 094002 (2013).
 - [15] R. N. Faustov and V. O. Gralkin, *Phys. Rev. D* **92** 054005 (2015).
 - [16] K. Miyahara, *Phys. Rev. C* **95** 035212 (2017).
 - [17] S. Kurokawa and E. Kikutani, *Nucl. Instrum. Methods Phys. Res. Sect. A* **499**, 1 (2003), and other papers included in this Volume; T.Abe *et al.*, *Prog. Theor. Exp. Phys.* **2013**, 03A001 (2013) and references therein.
 - [18] D. J. Lange, *Nucl. Instrum. Methods A* **462** 152 (2001).
 - [19] R. Brun, *et al.*, Report No. CERN DD/EE/84-1 (1984).
 - [20] A. Abashian *et al.* (Belle Collaboration), *Nucl. Instrum. Methods Phys. Res. Sect. A* **479**, 117 (2002); also see detector section in J.Brodzicka *et al.*, *Prog. Theor. Exp. Phys.* **2012**, 04D001 (2012).
 - [21] Z. Natkaniec *et al.* (Belle SVD2 Group), *Nucl. Instrum. Methods Phys. Res. Sect. A* **560**, 1 (2006).
 - [22] M. I. Adamovich *et al.* (WA99 Collaboration), *Eur. Phys. J. C* **5** 621 (1998).